

Synthetic wavelength based transportable telemeter with submicrometer resolution

Sheherazade Azouigui¹, Jean-Pierre Wallerand¹, Thomas Badr¹, Steven van den Berg²,
Marc Himbert¹ and Patrick Juncar¹

¹Laboratoire Commun de Métrologie LNE-CNAM, 61 rue du Landy, 93210 La Plaine Saint Denis, France.

²VSL, Thijsseweg 11, 2629 JA Delft, The Netherlands

Corresponding author: Jean-Pierre Wallerand

Abstract

We describe a transportable system based on synthetic wavelength interferometry for absolute distance measurement. The synthetic wavelength is generated using two frequency-doubled Nd:YAG lasers. Main feature is the elimination of polarization cross-talk issue using a setup where spatial separation is preferred to polarization separation. A superheterodyne technique has been implemented to detect the synthetic phase, enabling a fringe interpolation of $\sim 2\pi/5600$. A resolution of 700 nm over 60 s of integration time is demonstrated for a synthetic wavelength of 7,5 mm. An accuracy better than 10 μm is demonstrated over 25m, based on an indoor comparison with a classical fringe counting interferometer at VSL (Netherlands).

1 Introduction

Absolute long distance (ADM) measurements with high resolution are involved in many applications. Subnanometer resolution can easily be achieved with classical optical interferometry [1,2] but this method does not allow long-range and absolute distance measurements due to the short nonambiguity range (NAR) of $\pm \lambda/4$. Especially this technique is useless outdoor where measurements are worsened by mechanical vibrations and air index perturbations. Another alternative developed during the past twenty years is the synthetic wavelength interferometry (SWI)[3], which has shown to allow absolute distance measurement over several tens of meters with some 10^{-6} accuracy. The purpose of this technique is to generate a synthetic wavelength λ_s , much longer than the optical wavelength, resulting in an extended NAR and a reduced sensitivity to air index variations and mechanical vibrations.

In this work, SWI is achieved using two tunable frequency-doubled Nd:YAG lasers. A frequency separation of few GHz to 40 GHz between both lasers yields a synthetic wavelength of few mm to few cm. A superheterodyne detection of the synthetic phase is implemented [4]. The synthetic fringe order is determined for absolute measurement by tuning the synthetic wavelength. Contrary to classical systems, the system does not use polarization for beams separation, in order to avoid polarization-induced cyclic errors. Also, the setup has been built so that to be transportable. A submicrometer resolution is successfully achieved using a SW of ~ 7.5 mm. Indoor comparison of the system to a classical optical interferometer has resulted in an accuracy of ~ 4 μm over 25 m.

2 Experimental setup

2.1 Principle of the synthetic wavelength superheterodyne interferometer

Two-wavelength superheterodyne interferometry consists in injecting a Michelson-type interferometer with two beams of distinct frequencies ν_1 and ν_2 , separated by $\Delta\nu_s$ and measuring the synthetic phase, i.e. the phase difference between individual phases at ν_1 and ν_2 , given by:

$$\Phi_s = \Phi_2 - \Phi_1 = \frac{2\pi}{\Lambda_s} n_g D \quad (1)$$

where D is the optical path difference, n_g is the group refractive index written as:

$$n_g = \frac{n_2 \nu_2 - n_1 \nu_1}{\nu_2 - \nu_1} \quad (2)$$

n_1 and n_2 being phase indices respectively at frequency ν_1 and ν_2 .

Λ_s is the (vacuum) synthetic wavelength linked to the synthetic frequency $\Delta\nu_s$ by:

$$\Delta\nu_s = \nu_2 - \nu_1 = \frac{c}{\Lambda_s} \quad (3)$$

where c is the speed of light. Superheterodyne technique consists in generating for each beam of frequencies ν_1 and ν_2 , another beam which is slightly frequency shifted by f_1 and f_2 respectively. The detection of the synthetic phase is then performed at the superheterodyne frequency $\nu_2 - \nu_1$, with no need for separation of the different wavelengths. However the measured synthetic phase needs to be unwrapped by $2k\pi$, where k is the fringe order, i.e. the number of half synthetic wavelengths within the distance to be measured.

2.2 Synthetic wavelength superheterodyne interferometer

2.2.1 Optical setup

An ADM system has been built using a tunable SWI based on two frequency-doubled Nd:YAG lasers both emitting at 532 nm (see Figure 1). Owing to 60 GHz tunability of the optical frequencies ν_1 and ν_2 , a widely variable synthetic wavelength is enabled. A minimum value of 5 mm can be achieved with maximum frequency separation of 60 GHz between both lasers. One part of each green laser beam is injected in a single-mode fiber (FIB A) whereas the second part is slightly frequency-shifted by f_1 for laser 1 and by f_2 for laser 2 by means of acousto-optic modulators (AOM) before being coupled to a second single-mode fiber (FIB B). The superheterodyne frequency $\nu_2 - \nu_1$ is set at 50 kHz. The use of optical fibers allows the perfect superposition of the beams and also to separate the synthetic wavelength generation system from the measurement head (two distinct breadboards). Outputs of fibers A and B are linked to the measurement head. The probe signal consists in the beat note at the photodetector PDprobe of (1) beams of frequencies ν_i ($i=\{1;2\}$) pointed at the corner cube retroreflector and reflected back and (2) beams of frequencies $\nu_i + f_i$ directly pointed at PDprobe. A reference signal has also to be produced to cancel out phase fluctuations due to AOMs, optical fibers or uncommon paths between ν_1 and $\nu_1 + f_1$ (respectively ν_2 and $\nu_2 + f_2$). This is performed by detecting the beat note of part of the beams ν_i and $\nu_i + f_i$ with another photodetector (PDref). The measured phase difference of the probe and reference signals hence should only depend on the difference of optical distances travelled by beams $\nu_i + f_i$ and beams ν_i .

Important feature is that the designed system uses spatial separation rather than orthogonal polarizations to differentiate beams of frequencies ν_i from beams of frequencies $\nu_i + f_i$. This scheme allows to avoid periodic errors that could be introduced by cross-talk between S and P polarizations [5].

BREADBOARD 1

SW generation system

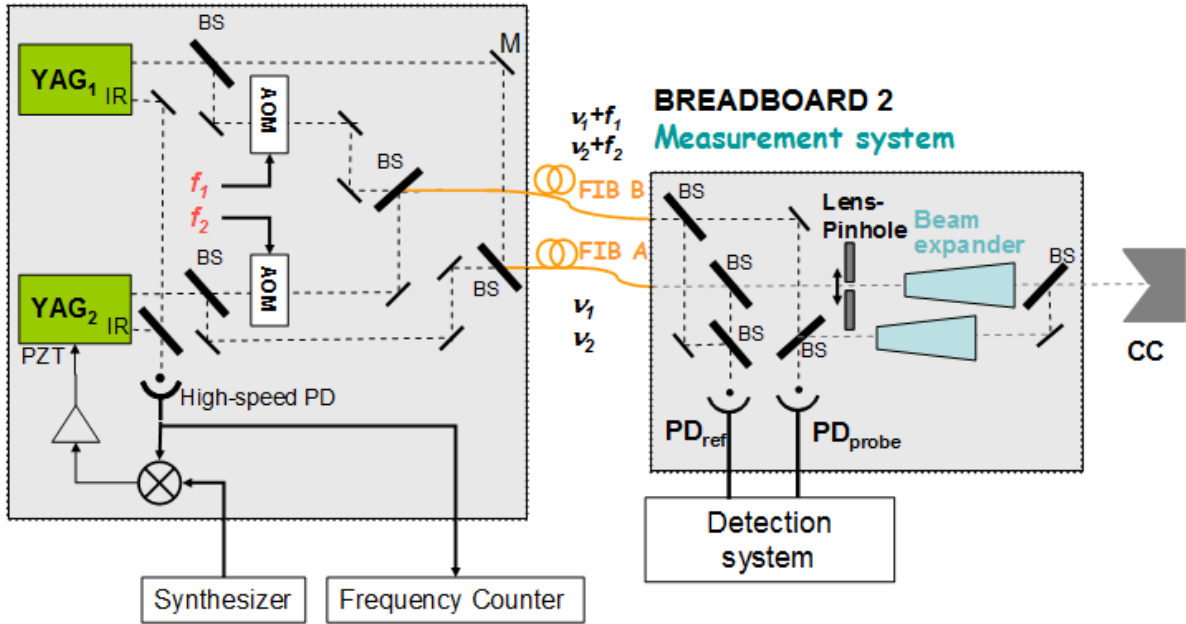


Figure 1: Optical setup for two-wavelength superheterodyne interferometer using frequency-doubled Nd:YAG lasers emitting at ~532 nm. AOM, acousto-optic modulator ; BS, beam splitter ; CC, hollow corner cube ; IR, infrared output ; M, mirror ; PDprobe, probe photodetector ; PDref, reference photodetector ; PZT, piezo-electric ceramic; SW, synthetic wavelength.



Figure 2 : SW generation system (breadboard 1 – dimensions: 0.45m x 0.60m)

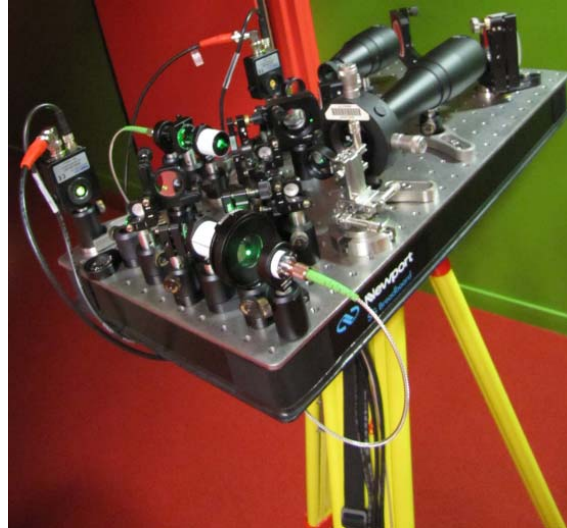


Figure 1 : Measurement head on tripod (breadboard 2 – dimensions: 0.3m x 0.6m)

2.2.2 Variation of the synthetic wavelength and phase-lock loop

The variation of synthetic wavelength (thus frequency) required for absolute distance measurement is automated under the software Labview. A voltage signal is first sent via one output of a data acquisition card to one of the lasers for temperature variation of the laser crystal to roughly reach the right synthetic frequency. Then a voltage signal is applied to the current control input of the laser power supply for fine adjustment. Finally a classical phase-lock loop enables to lock the frequency difference between both lasers to a reference frequency (Figure). This is performed by detecting the beat note of infrared outputs of the lasers at frequency $(\nu_2 - \nu_1)/2$ with a high-speed photodetector (New Focus 1417 Model , 25 GHz bandpass). This beat note is then mixed to a reference frequency (set at the desired infrared synthetic frequency) through a frequency mixer, whose IF output is sent to the piezo-electric ceramic (PZT) of one of the lasers after amplification and integration. The beating frequency is also detected by a frequency counter, referenced to a 10 MHz Rubidium clock. The relative accuracy of this reference is better than 10^{-10} and is the ultimate value that could be reached with our system.

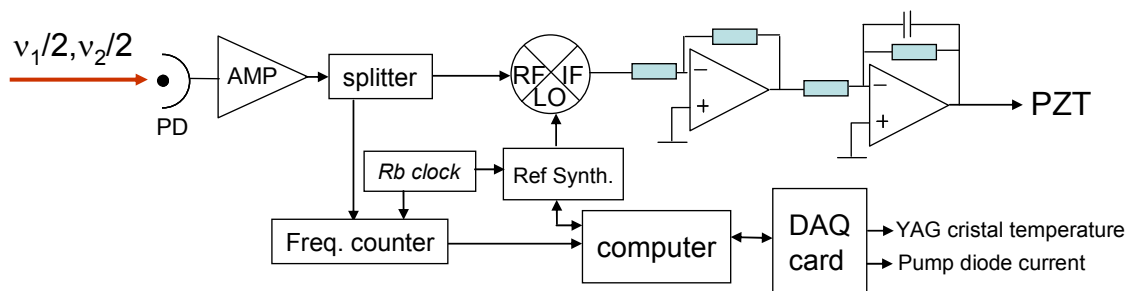


Figure 4 : Schematic of synthetic frequency variation, detection and lock in. AMP, amplifier ; DAQ, data acquisition ; PD, infrared photodetector ; PZT, piezo-electric ceramic.

2.3 Phase detection of the superheterodyne signal

The expression of probe and reference signals is detailed in [6]. The synthetic phase Φ_s is expressed as:

$$\Phi_s = (\Phi_{probe}(f_2) - \Phi_{probe}(f_1)) - (\Phi_{ref}(f_2) - \Phi_{ref}(f_1)) \quad (4)$$

where $\Phi_{probe}(f_1)$ (resp. $\Phi_{probe}(f_2)$) is the phase of the probe signal at frequency f_1 (resp. f_2) and $\Phi_{ref}(f_1)$ (resp. $\Phi_{ref}(f_2)$) is the phase of the reference signal at frequency f_1 (resp. f_2). The variation of the synthetic phase between two positions z_0 and z of the corner cube is given by:

$$\Phi_s(z) - \Phi_s(z_0) = \frac{4\pi}{c}(n_2\nu_2 - n_1\nu_1)(z - z_0) = \frac{4\pi}{c}n_g\Delta\nu_s L \quad (5)$$

Thus the distance $L=z-z_0$ between these positions can be extracted from the synthetic phase variation by:

$$L = \frac{\Phi_s(z) - \Phi_s(z_0)}{\frac{4\pi}{c}n_g\Delta\nu_s} \quad (6)$$

Figure 5 illustrates the superheterodyne system for detection of the synthetic phase. Probe and reference signals at PD_{probe} and PD_{ref} outputs are composed of signals at both frequencies f_1 and f_2 . Extraction of the synthetic phase at f_2-f_1 is usually performed by squaring signals using frequency mixers. In this work a different scheme is used to avoid significant variation of synthetic phase with optical power when using frequency mixers as squaring devices. Probe and reference signals are first down-frequency-shifted using frequency mixers and a local oscillator at frequency f_3 to obtain signals at frequencies f_2-f_3 (60 kHz) and f_1-f_3 (10 kHz). After electronic amplification these signals are sent to a data acquisition card for digital processing under Labview software. For both probe and reference signals the superheterodyne phase at 50 kHz is extracted from the phase between 10 kHz and 60 kHz tones, and the synthetic phase is then computed as the superheterodyne phase difference between both signals.

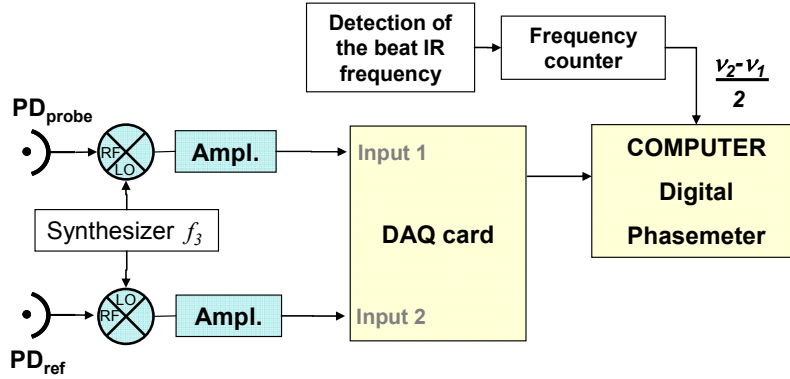


Figure 2 : Superheterodyne detection system: AMPL, amplifier ; PD_{probe}, probe photodetector ; PD_{ref}, reference photodetector ; IR, infrared ; RF, radio-frequency ; LO, local oscillator ; DAQ, data acquisition (5 Ms/sec, 12bits)

2.4 Compensation of the group index

The measured distance is corrected by the group refractive index n_g (Eq. (6)) which is determined by means of Edlén formulas using the measured temperature, pressure and humidity [7,8].

2.5 Determination of the fringe order

The system allows an absolute distance measurement, i.e. no incremental displacement of the corner cube retroreflector is needed. However the fringe order k must be determined since the measured value of the synthetic phase is in the interval $[-\pi;\pi]$ and needs to be unwrapped. This is simply performed by

measuring the synthetic phase for N values of the synthetic frequency and then by searching for coincidences for this set of N equations (Labview program).

3 Experimental results

3.1 Stability and resolution of the system

Figure 6 shows the Allan deviation of distance as a function of averaging time for a synthetic wavelength of ~ 7.5 mm (synthetic frequency of 40 GHz). As expected, the graph depicts a white frequency noise ($\sigma_y^2(\tau) \propto \frac{1}{\tau}$). Main result is the achievement of sub-micrometer resolution: a ~ 0.7 μm Allan deviation ($\sim 2\pi/5600$ fringe interpolation) is indeed obtained for 60 s averaging time.

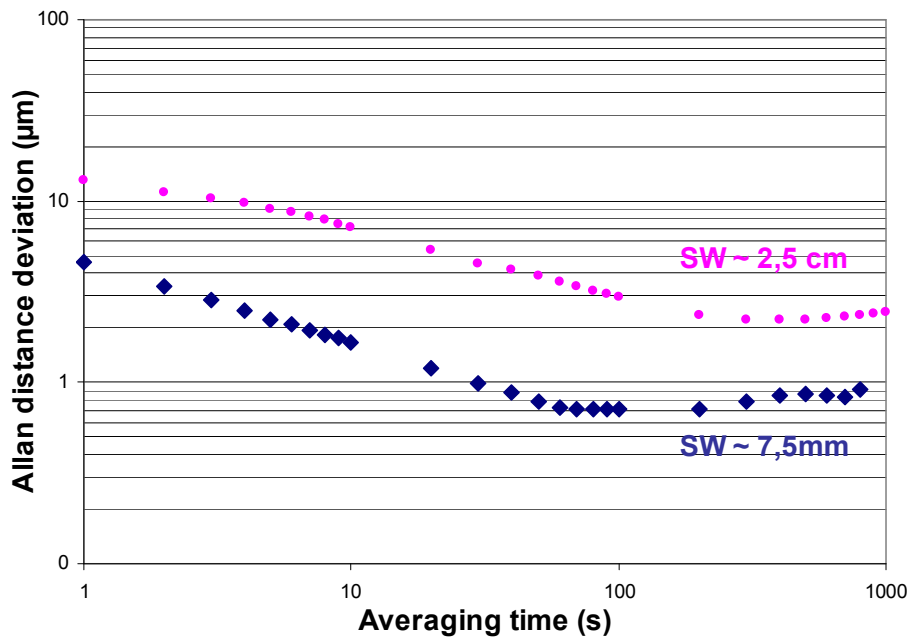


Figure 6 : Allan deviation of distance versus averaging time for $SW \sim 2.5$ cm ($\Delta\nu_s = 12$ GHz) and $SW \sim 7.5$ mm ($\Delta\nu_s = 40$ GHz)

Resolution has also been checked by performing measurements of micrometer order distances as depicted in Fehler! Verweisquelle konnte nicht gefunden werden.7. Displacement of the corner cube was realised with a micrometric displacement table. It was measured simultaneously with a counting fringe interferometer and with our distancemeter. Errors of measured values compared to those of the reference interferometer were below 0.3 μm . This figure thus confirms that the ADM system provides sub-micrometer resolution.

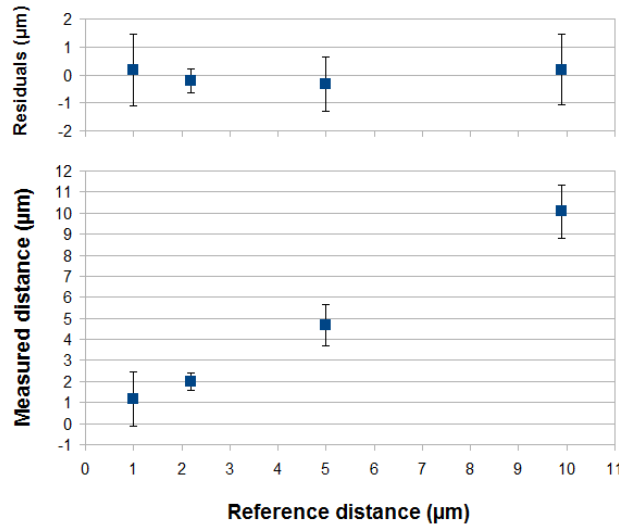


Figure 7 : Measured distance as a function of reference distance. Mean values of six measurements are represented with error bars corresponding to the standard deviation. Residuals correspond to the difference between classical interferometric measurement and our system.

3.2 Indoor comparison

The ADM system has been assessed indoor by comparison to a classical fringe counting (reference) interferometer (Spindler & Hoyer, He-Ne laser), over a 50m-long displacement bench at VSL (Delft, The Netherlands), in a temperature-controlled room. Measurements have consisted in following steps: (1) a zero position of the corner cube (CC) is measured at a point A (z_A) of the bench using the ADM system; (2) the CC is then moved from A to point B while the displacement is measured using the reference interferometer; (3) then the absolute distance is measured at B (z_B) using the ADM system. The distance between A and B ($z_B - z_A$) is then computed and compared to the value given by the reference interferometer. Absolute distance measurements have been performed using a synthetic frequency of 40 GHz (SW \sim 7.5mm) and a 10 s averaging time, yielding a \sim 2-3 μ m distance resolution. Then distance measurements have been carried out at several positions of the displacement bench from arbitrary zero positions up to 25 m (other 25 m of the bench were not available at that time) and repeated several times over the bench. Results of these measurements are given in Figure 8. Important feature is that results clearly reveal no increasing tendency of the error with distance. Figure 8 nevertheless shows that measurements are biased by $m_{res} \sim 4 \mu$ m with a standard deviation of $\sigma_{res} \sim 3 \mu$ m. If this observed bias can be interpreted in terms of reproducibility (which is not yet demonstrated), an accuracy of $\sim 4 \mu$ m can be assessed, computed as $\sqrt{m_{res}^2 + \sigma_{res}^2}$ ($k=1$). If interpreted in terms of systematic error, an accuracy of $\sim 10 \mu$ m ($k=2$), computed as $\frac{1}{2}(|m_{res}| + 2\sigma_{res})$ according to the practice of the European accreditation bodies.

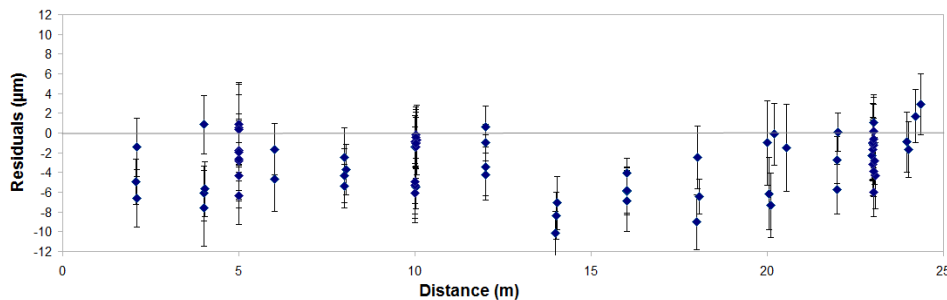


Figure 8 : Indoor comparison. Residuals of the measured distance with the ADM system compared to a fringe counting interferometer as a function of the distance.

4 Conclusion

A transportable absolute distance measurement system based on synthetic wavelength interferometry has been built. It allows us to achieve an angular resolution in the fringe pattern of $2\pi/5600$. The accuracy of the system was demonstrated to be better than $10\ \mu\text{m}$ along 25 m by comparison to an incremental He–Ne laser-based interferometer. No increasing tendency of the error with distance was detected so that this accuracy is certainly similar for longer distance. The implemented nonpolarized detection system avoids cyclic errors at this resolution scale. For the purpose of long distance outdoor measurements an improvement of the resolution is not necessary due to the limitation set by air index determination. Next step will be to implement a two-wavelength method using infrared and green outputs of YAG lasers [9] in order to compensate for air index in outdoor applications.

Acknowledgements

This work is part of the EURAMET joint research project “Long Distance”. It has received funding from the European Community’s Seventh Framework Programme, ERANET Plus, under Grant agreement 217257. Authors would like to thank the partners of the Long Distance project, particularly M. Zucco and M. Pisani from INRIM (Italy) for early measurements using INRIM 25-m-long displacement bench. Authors are also very grateful to Karl Meiners Hagen and Florian Pollinger from PTB (Germany) for very fruitful and open discussions.

References

- [1] F. C. Demarest 1998 High-resolution, high-speed, low data age uncertainty, heterodyne displacement measuring interferometer electronics, *Meas. Sci. Technol.* **9**, 1024
- [2] N. Bobroff 1993, Recent advances in displacement measuring Interferometry, *Meas. Sci. Technol.* **4**, 907
- [3] C. Polhemus Sep. 1973, Two-wavelength interferometry *Appl. Opt.*, vol. **12**, no. 9, pp. 2071–2074
- [4] R. Dandliker, R. Thalmann, and D. Prongué, May 1988 Two-wavelength laser interferometry using superheterodyne detection *Opt. Lett.*, vol. **13**, no. 5, pp. 339–341
- [5] C.-M. Wu and R. D. Deslattes, Oct. 1998 Analytical modeling of the periodic nonlinearity in heterodyne interferometry *Appl. Opt.*, vol. **37**, no. 28, pp. 6696–6700
- [6] S. Azouigui, T. Badr, J.-P. Wallerand, M. Himbert, J. Salgado and P. Juncar, 2010 Transportable distance measurement system based on superheterodyne interferometry using two phase-locked frequency-doubled Nd:YAG lasers, *Review of scientific instruments* **81**, 053112
- [7] P. E. Ciddor, Mar. 1996 Refractive index of air: New equations for the visible and near infrared,” *Appl. Opt.*, vol. **35**, no. 9, pp. 1566–1573
- [8] P. E. Ciddor and R. J. Hill, Mar. 1999 Refractive index of air. 2. Group index *Appl. Opt.* vol. **38**, no. 9, pp. 1663-1667
- [9] Karl Meiners-Hagen and Ahmed Abou-Zeid, 2008 Refractive index determination in length measurement by two-colour interferometry”, *Measurement Science and Technology* **19** 084004